

## BUCKLING BEHAVIOUR OF SHELLS USING AN AXISYMMETRICAL ELEMENT AND A TRIANGULAR ELEMENT

J.L. BATOZ, G. DHATT, J.P. PROST

*Civil Engineering Department,  
Université Laval, Cité Universitaire, Québec, G1K-7P4, Canada*

### SUMMARY

The purpose of this study is: (i) to develop a consistent axisymmetrical curved element for geometrically nonlinear shell problems; (ii) to present an efficient method for locating the unsymmetrical bifurcation paths along the symmetrical load displacement paths of axisymmetrical shells. It is of utmost importance to study the unsymmetrical bifurcations for shells undergoing snap-through type symmetrical buckling since these shells are very often sensitive to imperfections. (iii) to investigate the symmetrical and unsymmetrical pre- and post-buckling paths of axisymmetrical shells by a curved triangular element; (iv) and finally to compare the results obtained by these two elements and to evaluate their relative efficiency and reliability for predicting the symmetrical and unsymmetrical buckling loads. Also to compare these results with those obtained by other investigators, experimental and analytical.

The finite element formulation employs the Koiter-Sanders nonlinear strain displacement relations. For the axisymmetrical element, the displacements  $u$  and  $v$  are approximated by a quadratic polynomial (with a mid-point node) and  $w$  is approximated by a cubic polynomial for each harmonic. The nonlinear formulation employs the same interpolations. It may be mentioned that a consistent truncation error is obtained for linear and nonlinear energy functional by employing this element. The unsymmetrical bifurcations are initialised by introducing a load  $p(s, \theta) = p_0(1 + e \cos j\theta)$  where  $p_0$  is symmetrical load and  $e$  the perturbation load corresponding to harmonic " $j$ ". The bifurcation paths are systematically investigated for different values of " $j$ " as required in order to obtain the smallest load " $p$ ". The Newton-Raphson method is employed to solve the nonlinear relations. The residue is obtained by considering the coupling between symmetrical variables and the  $j$ -th harmonic variables. However, the tangent matrix is obtained by neglecting the coupling terms which reduces the bandwidth to half.

The symmetrical and unsymmetrical paths for similar shells are also studied by employing a triangular shallow element with 27 degrees of freedom, based on discrete Kirchhoff assumptions.

Each of these two elements are employed to study the following problems: (i) A number of circular cylindrical shells, subject to normal external pressure and hinged at both ends, are studied. Pre- and post-buckling behaviour is investigated for shells with different values of length, radius and thickness. (ii) The asymmetrical buckling pressures of truncated conical shells, subject to normal external pressure, are studied. For each case, the circumferential wave number " $j$ " corresponding to the lowest bifurcation load is obtained. These results compare favourably with those obtained by Famili (1965). (iii) The buckling loads corresponding to unsymmetrical bifurcations for clamped spherical shells, subject to uniform external pressure, are then studied. The circumferential wave number and imperfection sensitivity of these shells are obtained. The results have been compared with those obtained by Huang, Weinitschke, Famili and Archer.

A study of these problems have demonstrated that the axisymmetrical element may be effectively employed to initialise the unsymmetrical bifurcations. It has been also demonstrated that for the problems studied, the two elements give identical results.

INTRODUCTION

This paper deals with the investigation of pre- and post-buckling symmetrical and asymmetrical behaviour of cylindrical spherical and conical thin shells with linear elastic properties.

The main features of this study are stated as follows: (i) A consistent axisymmetrical curved element is developed for geometrically nonlinear shell problems. An efficient method of tracing unsymmetrical bifurcation paths for axisymmetrical shell problems is then presented. (ii) A triangular curved element is applied to investigate the symmetrical and unsymmetrical pre- and post-buckling paths of axisymmetrical shells. A triangular finite element model is obtained for each problem in such a manner that the symmetrical nature of the solution is fully exploited in order to reduce problem size. (iii) Finally, the results obtained by these two elements for different problems are compared in order to evaluate their relative reliability and efficiency.

AXISYMMETRIC CURVED ELEMENT

A large number of researchers (8,11,12,13,17,18) employed different types of axisymmetrical elements for studying linear and nonlinear behaviour of thin shells of revolution. An exhaustive survey presented by Svalbonas (19) may be consulted for further reference.

The problem size for studying nonlinear behaviour of axisymmetrically loaded shells increases considerably as compared with the corresponding linear problem, due to couplings among various harmonic components. Stricklin et al. (18) and Haisler (9) have presented a numerical method for studying such nonlinear problems.

For any reliable estimate of buckling loads of axisymmetrically loaded shells, one must not only investigate the pre- and post-buckling axisymmetrical behaviour but also the asymmetrical bifurcation paths. According to authors' knowledge, little work has been reported in this direction by using the finite element method. The formulation and results presented herein are a contribution in this field.

Strain Displacement Relations: These are given by Sanders (15) where the strains (e,k) and products of rotations ( $\psi_s^2, \psi_\theta^2, \psi_s \psi_\theta, \psi_{s\theta}^2$ ) are assumed small and displacements (u,v,w) are assumed large. The midsurface strains and changes of curvature are defined by:

$$e = \begin{bmatrix} u_{,s} - w \phi_{,s} + \frac{1}{2}(\psi_s^2 + \psi_{s\theta}^2) \\ \frac{1}{r} (u \sin \phi + v_{,\theta} + w \cos \phi) + \frac{1}{2} (\psi_\theta^2 + \psi_{s\theta}^2) \\ \frac{1}{r} (r v_{,s} + u_{,\theta} - v \sin \phi) + \psi_s \psi_\theta \end{bmatrix}$$

$$k = \begin{bmatrix} \Psi_{s,s} \\ \frac{1}{r} (\Psi_{\theta,\theta} + \Psi_s \sin \phi) \\ \Psi_{\theta,s} + \frac{1}{r} \Psi_{s,\theta} - \Psi_\theta \frac{\sin \phi}{r} + (\phi_{,s} + \frac{\cos \phi}{r}) \Psi_{,s\theta} \end{bmatrix} \quad (1)$$

where  $\Psi_s = -(w_{,s} + u \phi_{,s})$ ;  $\Psi_\theta = -\frac{1}{r} (w_{,\theta} - v \sin \phi)$ ;  $\Psi_{s\theta} = \frac{1}{2r} (r v_{,s} + v \sin \phi - u_{,\theta})$   
 $u_{,s} = \partial u / \partial s$ ,  $\phi_{,s} = \partial \phi / \partial s$  etc.

The total strain vector at a point of the shell element is defined by:

$$\epsilon = e + \xi k \quad \text{where } -h/2 \leq \xi \leq h/2 \text{ and } h \text{ is the thickness of the shell.}$$

Finite Element Formulation: A shell of revolution is discretised by a number of curved axisymmetrical elements as shown in Fig. 1. A quadratic variation of the slope of the middle surface is assumed along the meridional direction as given in ref. 17. The choice of the interpolation functions for displacements  $u, v$  and  $w$  is based on the assumption that all three components play an equally important role in predicting the shell behaviour. This leads to the following set of consistent interpolation functions.

$$\begin{aligned} u(s, \theta) &= \sum_{j=0}^n (a_1^j + a_2^j s + b_1^j s (s-l)) \cos j\theta \\ v(s, \theta) &= \sum_{j=0}^n (a_3^j + a_4^j s + b_2^j s (s-l)) \sin j\theta \\ w(s, \theta) &= \sum_{j=0}^n (a_5^j + a_6^j s + a_7^j s^2 + a_8^j s^3) \cos j\theta \end{aligned} \quad (2)$$

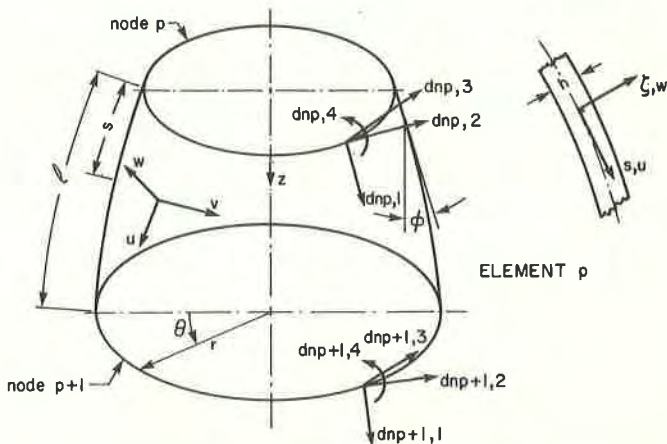


Fig. 1 — AXISYMMETRICAL CURVED ELEMENT.

where  $s, \theta$  are the meridional and circumferential coordinates,  $l$  is the length of the element and coefficients  $b_1, b_2$  are eliminated by static condensation.

An element having eight degrees of freedom for each harmonic 'j' is obtained where four variables ( $u, v, w, w_s + u\phi_s$ ) are assigned with each of the two nodes. The assembled equilibrium relations for a finite element model are obtained in a routine manner from the stationary conditions of the potential energy functional, once the relations (1) and (2) are defined. The equilibrium equations may be written as:

$$(K d_n - F) = R = 0 \quad (3)$$

where  $K$  is the nonlinear equilibrium matrix,  $d_n$  is the total nodal displacement vector and  $F$  is the equivalent load vector. Eq. (3) includes all harmonic components, which are considered at any one time, and their couplings. These relations are solved by the Newton Raphson method (1). The incremental form of this method is given by:

$$K_v \Delta d_n + R = 0 \quad (4)$$

The details of the matrices  $K$  and  $K_v$  are given in the reference (14). In general, the matrix  $K_v$  contains all harmonics and its couplings. In order to keep the computation efforts for solving Eq.(3) within realistic limits, the following simplifications are introduced. (i) At any one time, only two harmonics are considered, i.e. axisymmetrical mode  $j=0$  and a harmonic mode 'j'. (ii) All the harmonic coupling terms are considered in Eq.(3) whereas harmonic couplings are completely neglected in Eq.(4) which is written as:

$$\begin{bmatrix} K_v^0 & 0 \\ 0 & K_v^j \end{bmatrix} \begin{bmatrix} \Delta d_n^0 \\ \Delta d_n^j \end{bmatrix} + \begin{bmatrix} R^0 \\ R^j \end{bmatrix} = 0 \quad (5)$$

It may be remarked that a convergent solution obtained by solving Eq.(5) will seek to satisfy Eq.(3) where harmonic couplings are fully considered.

#### CURVED TRIANGULAR ELEMENT

The formulation of the 27 D.F. element, based on the discrete Kirchhoff assumptions, has been reported in the references (1) and (2). The strain displacement relations employed are those given by Sanders (15). The assumptions of small strains, moderate rotations and large displacements are respected. However, the rotation about the normal is neglected compared to the other two rotations. For a given shell problem the finite element model is obtained in such a manner that the symmetrical properties of the solution

(i.e. displacements) are fully exploited to reduce the problem size. For axisymmetrical problems, a segment of shell, having an angle of  $\pi/N$  at its base is discretised by a set of finite elements (Fig. 2a) where 'N' represents the number of elements along the meridional or axial direction. Symmetrical conditions are then introduced over the nodes so that desired displacement modes are fully simulated. The introduction of symmetrical conditions will require rotations of variables in the tangent plane of a shell surface. This technique has been applied by Cowper et al. (3) for linear axisymmetrical problems. In this paper, it is applied first to solve nonlinear axisymmetrical problems and then is generalised in such a manner that any asymmetrical displacement mode may be simulated. In order to represent the zero and j'th harmonic (and its multiples) modes, a finite element model for a shell segment having an angle of  $\pi/j$  at its base is obtained. This is shown for various shells in Fig. 2.

#### SOLUTION METHOD AND UNSYMMETRICAL BIFURCATIONS

The Newton Raphson method as described in Ref.(1) is applied to solve the system of nonlinear equations. The unsymmetrical bifurcation paths are initialised and traced in a manner similar to that discussed in (1). The following remarks may be presented which are relevant to the two elements employed in this study.

Axisymmetrical Element: It is assumed that unsymmetrical bifurcations are fully represented by a single harmonic mode and the axisymmetrical mode. The nonlinear load displacement path is traced upto a certain load without considering a harmonic. If it is desired to investigate the unsymmetrical bifurcation around a load level, a harmonic mode is chosen which is assumed to be most dominant. A perturbation load corresponding to this harmonic is then introduced along with the axisymmetrical load. The magnitude of the perturbation load is about 1% of the given load. The solution is then continued under the unsymmetrical loading condition. If there is an unsymmetrical bifurcation, it will be observed by a bifurcation in the load displacement curve. If so, the perturbation load may be removed and the asymmetrical path may be traced corresponding to different values of axisymmetrical load. If it is of interest to investigate the bifurcations for another harmonic mode, the same process is repeated.

Triangular Element: It is assumed that unsymmetrical displacements are fully represented by an axisymmetrical mode and a harmonic 'j' or its multiples. A finite element model for a portion of shell having an angle of  $\pi/j$  at its base is thereby obtained (Fig. 2). The symmetrical conditions on various nodes are introduced in such a manner that the desired harmonic mode or its multiples and the axisymmetrical displacements are exactly simulated. The nonlinear load displacement relations are traced up to a certain axisymmetrical load level. To initialise unsymmetrical bifurcations, a concentrated perturbation load is applied at a node, not located symmetrically in the finite element mesh. The magnitude of the perturbation load may vary from 1% to 30% of the corresponding axisymmetrical load at that node. An unsymmetrical solution for this combined load level is then obtained. The

perturbation load is removed and the Newton Raphson solution technique is continued by using the unsymmetrical displacement thus calculated as an initial estimate. If the solution converges to the asymmetrical mode, for the given axisymmetrical load level, the entire path may be traced. If not, it is assumed that no bifurcations exist at this level, corresponding to the chosen harmonic mode or its multiples. The search may be continued for different load levels for a chosen harmonic mode. In order to investigate bifurcations corresponding to another harmonic mode, a finite element model for the corresponding shell segment is chosen and the process as discussed above is repeated.

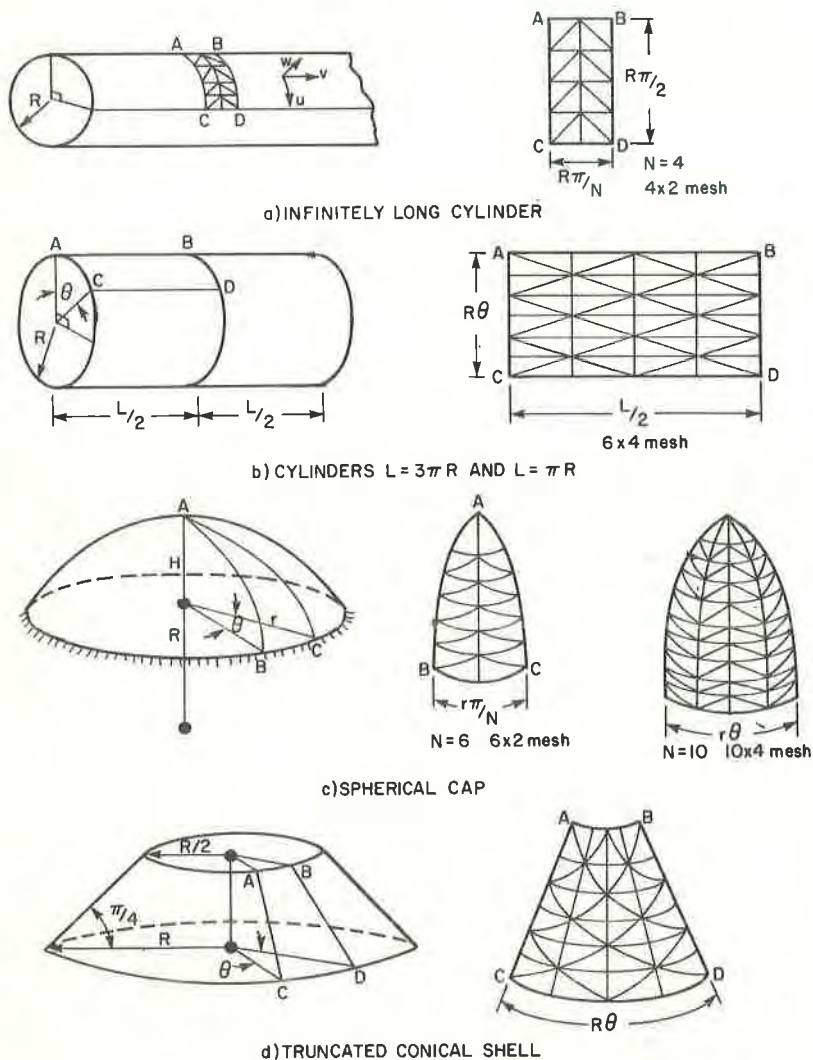


Fig. 2 — TYPICAL MESHES USED WITH THE TRIANGULAR SHELL ELEMENT.

RESULTS

A number of cylindrical, spherical and truncated conical shells, subject to uniform external pressure remaining normal to the undeformed surface, are analysed with two types of elements.

Thin Circular Cylinders: The estimates of buckling loads of three simply supported cylinders are obtained by triangular and axisymmetrical elements. The values of critical load parameter  $K_y = P_{crit} R^3/D$ , along with shell properties, are given in the Table I where results obtained by Simitzes and Aswani (16) and by Flugge are also reported. Flugge's results correspond to nonconservative loading which remain normal to the deformed surface. The mesh configurations for triangular elements are shown in Figs. 2a and 2b. A convergence study of buckling loads for different triangular mesh sizes, harmonic modes and sizes of shell sectors is also given in the Table I. The corresponding results employing the axisymmetrical element are also reported therein. It may be noted that the cylindrical shells have a basically linear pre-buckling axisymmetrical behaviour. Only a very small amount of asymmetrical perturbation load is necessary to initialise bifurcations for the two elements employed.

Clamped Spherical Shells: Two clamped spherical caps, subject to uniform external pressure (Figs. 2c, 3, 4), are studied. These shells have the following geometrical parameters:

$$S1: \lambda = (3(1 - \nu^2))^{1/4} (H/h)^{1/2} = 6 ; R/h = 400; \nu = 1/3$$

$$S2: \lambda = 15 ; R/h = 2500; \nu = 1/3$$

where H is defined in Fig. 2c.

The axisymmetrical nonlinear behaviour of S1 and S2 shells is obtained by using 6 x 2 and 10 x 2 meshes respectively with the triangular element (Fig. 2c) whereas 8 and 16 axisymmetrical elements are employed for the corresponding cases. The asymmetrical bifurcation paths are obtained by using 6 x 6 mesh over a quarter of S1 ( $\theta = \pi/2$ ) and 10 x 4 mesh over a sector of S2 having  $\theta = \pi/10$ , and 8 axisymmetrical elements are used for both shells. The symmetrical and asymmetrical nonlinear load displacements paths for S1 and S2 are given in Fig. 3 and Fig. 4 respectively. The normal displacements at the pole and at the middle of the meridian are chosen for comparison for S1 whereas the load displacement history for the points B and C (Fig. 4) is given for S2.

The results obtained by using the triangular and axisymmetrical elements, and those reported by Famili & Archer (5), Fitch & Budiansky (6), Huang (10) and Weinitschke (20), show excellent agreement as may be seen from Figs. 3 and 4. The bifurcation buckling loads for different harmonic modes as calculated with the axisymmetrical element are also compared with those given by Huang (10) (Figs. 3 and 4). The variation of moment  $M_s$  and the stress  $N_s$  for S2 along meridional direction for different values of  $\theta$  are shown in Fig. 4.

This corresponds to the load level of  $P/P_0 = 0.72$  in the asymmetric post-buckled zone for 10th harmonic mode. One may observe that the buckled zone is located near the clamped edge.

Truncated Conical Shells: Two simply supported truncated conical shells, subject to uniform normal pressure, are studied. The base angle is  $45^\circ$  and taper ratio  $\psi$  is 0.5.

$$C1: \lambda^2 = (12(1 - \nu^2))^{1/2} \cdot R \cdot \sqrt{2}/h = 121.24 \quad \nu = 0.3$$

$$C2: \lambda^2 = 277.13 \quad \nu = 0.3$$

where  $R$  is radius of curvature at the base (Fig. 2d). The results for different mesh sizes and harmonic modes using the two elements are given in the Table II. These are compared with those obtained by Niordson and Famili in the reference (4). It has been observed that the shells have basically a linear pre-buckling behaviour. The present results show better agreement with those of Niordson than with those of Famili. It seems that a finer triangular element mesh would be required to obtain results of precision comparable to the axisymmetrical element. However the disparity among different results given in the Table II is still open to question and a further investigation is necessary in order to give satisfactory explanations.

#### CONCLUDING REMARKS

The triangular element has been employed to study asymmetrical buckling behaviour of various types of shells of revolution. A method has been presented to exploit the symmetry properties for reducing the problem size. The method to obtain asymmetrical bifurcation paths by using the axisymmetrical element has been presented and thoroughly tested. Various comparisons presented have demonstrated the reliability and capability of the application of these two types of elements for asymmetrical shell bifurcations.



REFERENCES

1. Batoz, J.L., Chattopadhyay, A. & Dhatt, G., "Finite Element Large Deflection Analysis of Shallow Shells", to be published in Int. J. Num. Meth. Engg., 1975.
2. Batoz, J.L. & Dhatt G., "Buckling of Deep Shells", Proceedings of the 2nd Int. Conf. on "Struc. Mech. Reactor Tech.", Berlin, Germany, 10-14 Sept. 1973, Vol. V, Part M, M5/7, pp. 1-12.
3. Cowper, R., Lindberg, G.M. & Olson, M.D., "Comparison of Two-High-Precision Triangular Finite Element for Arbitrary Deep Shells", Proc. 3rd Conf. Matrix Meth. in Struc. Mech., WPAFB, Ohio, Oct. 1971, pp. 277-304.
4. Famili, J., "Asymmetric Buckling of Finitely Deformed Conical Shells", AIAA J., Vol. 3, no. 8, Aug. 1965, pp. 1456-1461.
5. Famili, J. & Archer, R.R., "Finite Asymmetric Deformation of Shallow Spherical Shells", AIAA J., Vol. 3, no. 3, March 1965, pp. 506-510.
6. Fitch, J.R. & Budiansky, B., "Buckling and Postbuckling Behavior of Spherical Caps under Axisymmetric Load", AIAA J., Vol. 8, no. 4, April 1970, pp. 686-693.
7. Flügge, W., "Stresses in Shells", 2nd. Edition, Springer-Verlag, New-York, Heidelberg, Berlin 1973, pp. 459-463.
8. Grafton, P.E. & Strome, D.R., "Analysis of Axisymmetric Shells by the Direct Stiffness Method", AIAA J., Vol. 1, no. 10, Oct. 1963, pp. 2343-2347.
9. Haisler, W.E. Jr., "Development and Evaluation of Solution Procedures for Nonlinear Structural Analysis", Ph. Thesis, Aerospace Engg. Dept., Texas A. & M. Univ., Dec. 1970.
10. Huang, N.C., "Unsymmetrical Buckling of Thin Shallow Spherical Shells", J. Appl. Mech., Vol. 31, no. 4, Sept. 1964, pp. 447-457.
11. Jones, R.E. & Strome, D.R., "Direct Stiffness Method Analysis of Shells of Revolution Utilizing Curved Element", AIAA J., Vol. 4, no. 9, Sept. 1966, pp. 1519-1525.
12. Navaratna, D.R., Pian, T.H.H. & Witmer, E.A., "Stability Analysis of Shells of Revolution by the Finite Element Method", AIAA J., Vol. 6, no. 2, Feb. 1968, pp. 355-361.
13. Percy, J.H., Pian, T.H.H., Klein S. & Navaratna, D.R., "Application of Matrix Displacement Method to Linear Elastic Analysis of Shells of Revolution", AIAA J., Vol. 3, no. 11, Nov. 1965, pp. 2138-2145.
14. Prost, J.P., "Developpement d'un élément axisymétrique pour l'étude de la stabilité élastique des voiles minces de révolution", Thèse de Maîtrise, Génie Civil, Univ. Laval, Québec, Canada, 1975.
15. Sanders, J.L. Jr., "Nonlinear Theories for Thin Shells", Quart. Appl. Math., Vol. 21, pp. 21-36, 1963.
16. Simitzes, G.J. & Aswani, M., "Buckling of Thin Cylinders under Uniform Lateral Loading", J. Appl. Mech., Vol. 41, no. 4, Sept. 1974, pp. 827-829.
17. Stricklin, J.A., Navaratna, D.R. & Pian, T.H.H., "Improvements on the Analysis of Shells of Revolution by the Matrix Displacement Method", AIAA J., Vol. 4, no. 11, Nov. 1966, pp. 2069-2072.
18. Stricklin, J.A., Haisler, W.E., Mac Dougall, H.R. & Stebbins, F.J., "Nonlinear Analysis of Shells of Revolution by the Matrix Displacement Method", AIAA J., Vol. 6, no. 12, Dec. 1968, pp. 2306-2312.
19. Svalbonas, V., "Numerical Analysis of Stiffened Shells of Revolution", NASA-CR-2273, Vol. 1, Sept. 1973, pp. 6-11.
20. Weinitschke, H.J., "On Asymmetric Buckling of Shallow Spherical Shells", J. Math. Phys., Vol. 44, no. 2, 1965, pp. 141-163.

| C1: Infinitely Long Cylinder, $R/h = 100$ , $\nu = 1/3$ |                                |                           |        |
|---|--------------------------------|---------------------------|--------|
| Element Employed  | mesh, harmonic j               | $\frac{P_{crit.} R^3}{D}$ | Error* |
| Triangular Element                                      | 4x2 mesh, $\theta=\pi/2$ ; j=2 | 4.268                     | 6.7%   |
|   | 6x2 mesh, $\theta=\pi/2$ ; j=2 | 4.084                     | 2.0%   |
| Axisymmetrical Element                                  | 1 element, j=2                 | 3.85                      | 3.7%   |
| Simitzes and Aswani (Ref. 16) j=2                       |                                | 4.00                      |        |
| Flügge (Ref. 7)** j=2                                   |                                | 3.00                      |        |
| C2: Cylinder $L = 3\pi R$ , $R/h = 200$ , $\nu = 1/3$   |                                |                           |        |
| Triangular Element                                      | 4x4 mesh, $\theta=\pi/2$ ; j=4 | 21.76                     | 23.0%  |
|   | 6x4 mesh, $\theta=\pi/2$ ; j=4 | 18.41                     | 4.1%   |
|   | 6x4 mesh, $\theta=\pi/4$ ; j=4 | 18.218                    | 3.0%   |
| Axisymmetrical Element                                  | 8 elements, $L/2$ , j=4        | 17.665                    | 0.1%   |
|   | 8 elements, $L/2$ , j=3        | 18.132                    |        |
| Simitzes and Aswani (Ref. 16) j=4                       |                                | 17.68                     |        |
| Flügge (Ref. 7)** j=4                                   |                                | 16.21                     |        |
| C3: Cylinder $L = \pi R$ , $R/h = 1000$ , $\nu = 1/3$   |                                |                           |        |
| Triangular Element                                      | 6x4 mesh, $\theta=\pi/2$       | 181.76                    | 75.0%  |
|   | 6x4 mesh, $\theta=\pi/4$ ; j=8 | 111.57                    | 8.0%   |
|   | 6x4 mesh, $\theta=\pi/8$ ; j=8 | 110.18                    | 6.7%   |
|   | 6x4 mesh, $\theta=\pi/9$ ; j=9 | 105.34                    | 2.0%   |
| Axisymmetrical Element                                  | 5 elements, $L/2$ , j=9        | 103.08                    | 0.3%   |
| Simitzes and Aswani (Ref. 16) j=9                       |                                | 103.34                    |        |
| Flügge (Ref. 7)** j=9                                   |                                | 101.98                    |        |

\* Error with respect to Simitzes and Aswani's solution (16)

\*\* Non conservative loads remaining normal to the deformed surface.

$$D = Eh^3/12 (1 - \nu^2)$$

TABLE 1: Cylindrical Shells\_Buckling Loads

| Conical Shell, $\alpha = 45^\circ$ , $\Psi = 0.5$ , $\nu = 0.3$ , $\lambda^2 = 121.24$ |  |                |
|--|--|----------------|
| Element Employed   | mesh, harmonic j                         | P              |
| Triangular Element   | 4x6 mesh, $\theta = \frac{\pi}{5}$ , j=5 | 154            |
| Axisymmetrical Element   | 6 elements, j=4<br>6 elements, j=5       | 132<br>125     |
| Famili (Ref. 4)  | j=4                                      | 89.75          |
| Niordson (from Ref.4)  | j=5                                      | 121            |
| Conical Shell, $\alpha = 45^\circ$ , $\Psi = 0.5$ , $\nu = 0.3$ , $\lambda^2 = 277.13$ |  |                |
| Triangular Element   | 4x6 mesh, $\theta = \frac{\pi}{6}$ , j=6 | 203            |
| Axisymmetrical Element   | 6 elements, j=6<br>6 elements, j=7       | 188.6<br>188.5 |
| Famili (Ref. 4)  | j=6                                      | 143.8          |
| Niordson (from Ref. 4)   | j=6                                      | 173            |

$\lambda^2 = [12 (1-\nu^2)]^{\frac{1}{2}} \cdot R \sqrt{Z}/h \quad (\alpha=45^\circ)$   
 $\Psi = 1 - R/2R = 0.5 \quad \text{taper ratio}$   
 $P = [12 (1-\nu^2) \cdot R^3 \cdot \sqrt{Z}/h^3] \cdot p/E$   
 $\nu$  : Poisson's ratio, E: modulus of Elasticity  
 $h$  : thickness, p: uniform external pressure  
 $R$  : maximum radius (Fig. 2)

TABLE 2: Truncated Conical Shells - Buckling Loads

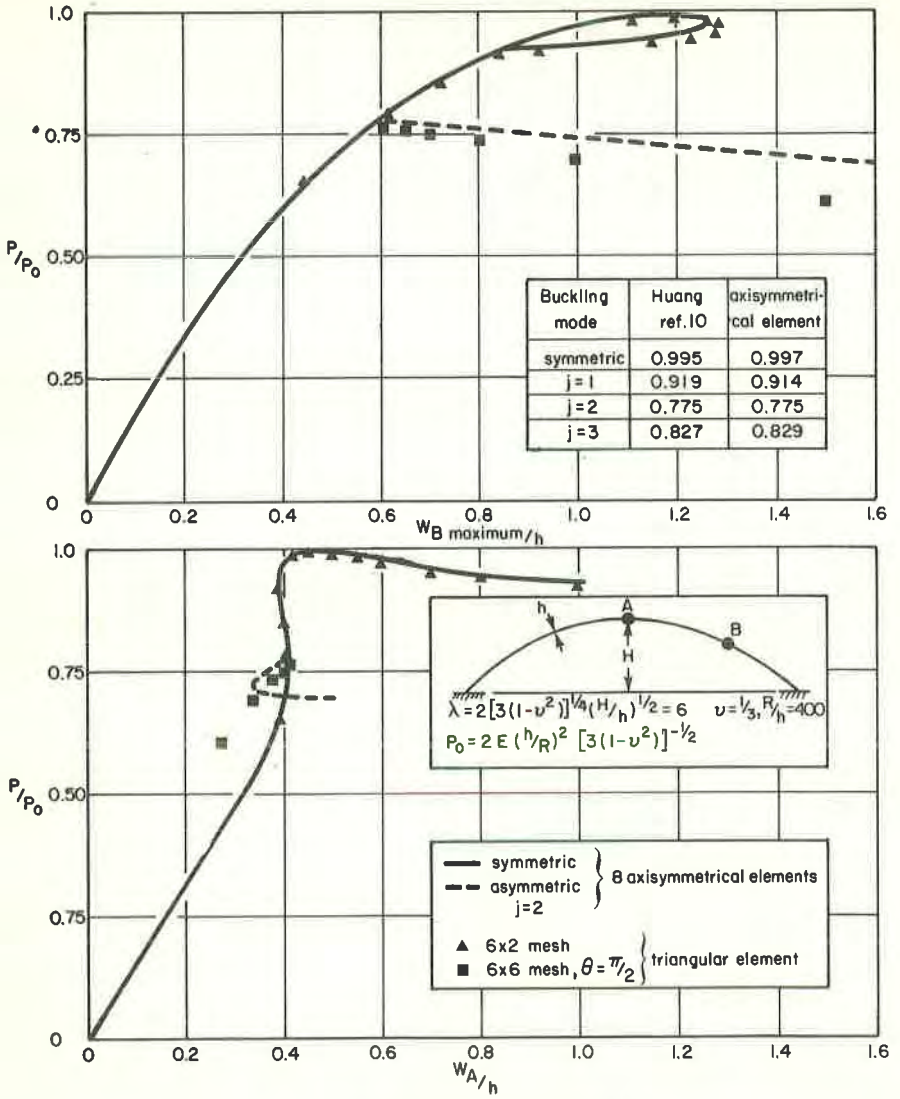
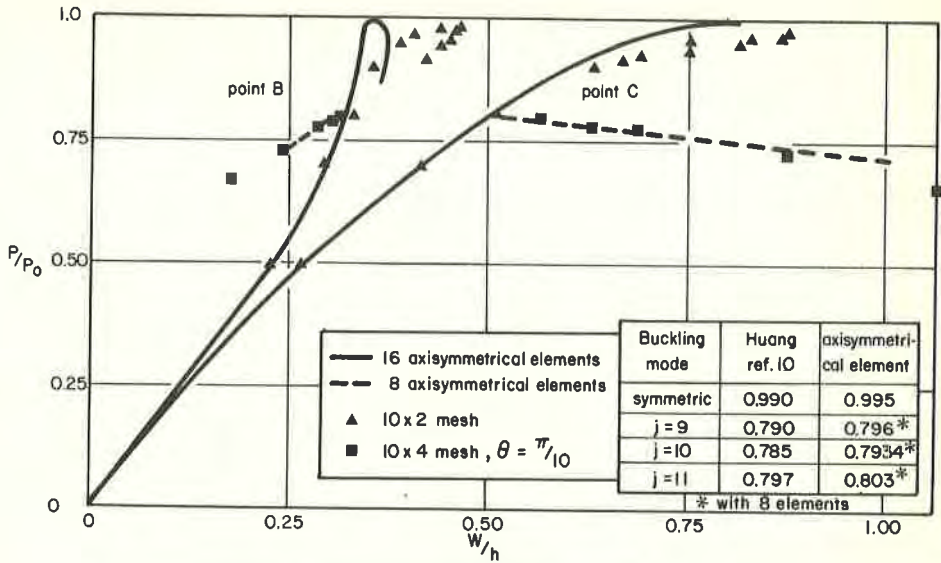
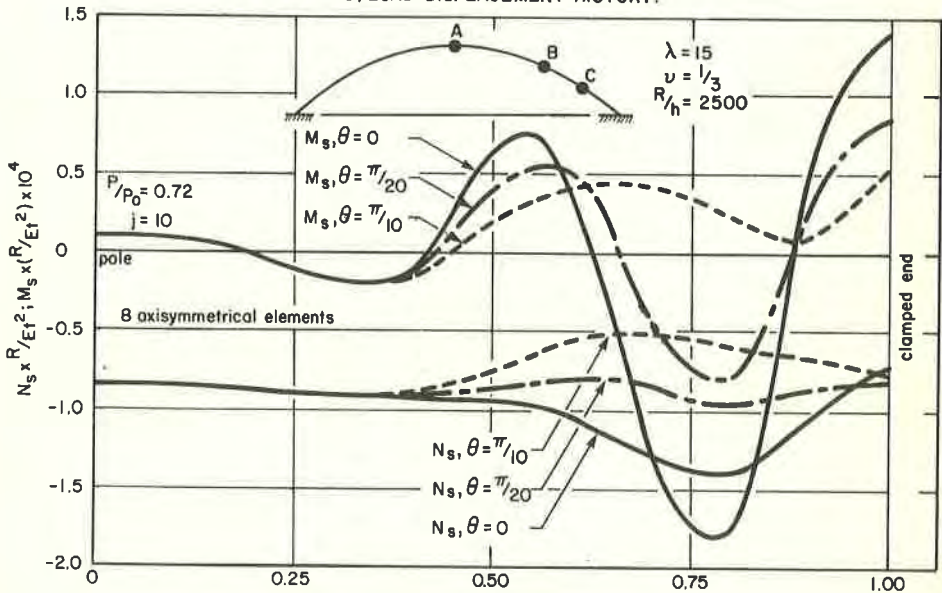


Fig. 3 — SPHERICAL SHELL SI.



a) LOAD-DISPLACEMENT HISTORY.



b) VARIATIONS OF  $M_s$  AND  $N_s$  ALONG THE MERIDIAN AFTER BUCKLING.

Fig. 4 — SPHERICAL SHELL S2.

